

Mechanical Properties of Spider Silk at Cryogenic Temperatures

Jivan Kurinec

*Mechanical Properties of Spider Silk
at Cryogenic Temperatures*

By

Jivan Kurinec
Rush-Henrietta Senior High School
Henrietta, New York

Supervised by

Mr. Mark Bonino
Dr. David R. Harding

High School Research Program
Laboratory for Laser Energetics
University of Rochester
Rochester, NY

Summer 2004

Table of Contents

Abstract.....	1
I. Introduction.....	1
1.1 Laboratory for Laser Energetics (LLE).....	1
1.2 The OMEGA System.....	2
1.3 The Fusion Reaction.....	2
1.4 Inertial Confinement Fusion (ICF).....	4
1.5 Spider Silk.....	5
1.6 Application of Spider Silk in Inertial Confinement Fusion (ICF).....	5
1.7 Mechanical Properties.....	6
1.8 Mechanical Properties of Spider Silk.....	10
II. Objective.....	11
III. Experimental.....	11
3.1 Silk Sample.....	11
3.2 Sample Mounting.....	12
3.3 Sample Testing.....	12
IV. Results and Discussion.....	15
4.1 Silk Diameter.....	15
4.2 Stress-Strain Characteristics.....	15
V. Conclusions.....	17
Acknowledgments.....	17
References.....	18

Mechanical Properties of Spider Silk at Cryogenic Temperatures

Jivan Kurinec
Rush-Henrietta High School
Laboratory for Laser Energetics
University of Rochester, Rochester, New York

ABSTRACT

The work presented in this study was carried out as part of the High School Research Program at the Laboratory for Laser Energetics (LLE), University of Rochester during the summer of 2004. In this study, mechanical properties of dragline spider silk fiber were measured at temperatures of 293K and 158K for target mount applications in Inertial Confinement Fusion (ICF). This interest in dragline spider silk is due to its impressive mechanical properties that combine both a high tensile strength and a high elasticity. A Thermal Mechanical Analyzer system was used to apply force with high precision (~ 0.1 mN) and measure extremely small displacements ($\sim 0.1 \mu\text{m}$). Important mechanical properties - Young's Modulus (stiffness), ultimate tensile strength (UTS) and ultimate tensile strain were determined. The results show that there is little variance in the ultimate tensile strength (UTS) and ultimate strain from room temperature to 158K, whereas the stiffness of the silk increased by a factor of two. These observations demonstrate that the spider silk maintains its desirable elastic properties at cryogenic temperatures for ICF target mount application.

I. INTRODUCTION

1.1 Laboratory for Laser Energetics (LLE)

The Laboratory for Laser Energetics (LLE) at University of Rochester was established in 1970 to investigate the interaction of high power lasers with matter. LLE is a national

resource for conducting implosion experiments in support of the National Inertial Confinement Fusion (ICF) program [1]. Available at the LLE for National Laser User Facility (NLUF) researchers is the OMEGA laser, a 30-kJ UV 60-beam laser system (at 35 nm) suitable for direct-drive ICF implosions.

1.2 The OMEGA System

OMEGA (see Fig.1) stands 10 meters tall and is approximately 100 meters in length [2]. This system delivers pulses of laser energy to targets in order to measure the resulting nuclear and fluid dynamic events. OMEGA's 60 laser beams focus up to 40,000 joules of energy onto a target that measures less than 1 millimeter in diameter in approximately one billionth of a second [2]. At LLE scientists continue to research what will one day become a vast source of power using the ocean's abounding storehouse of potential energy.

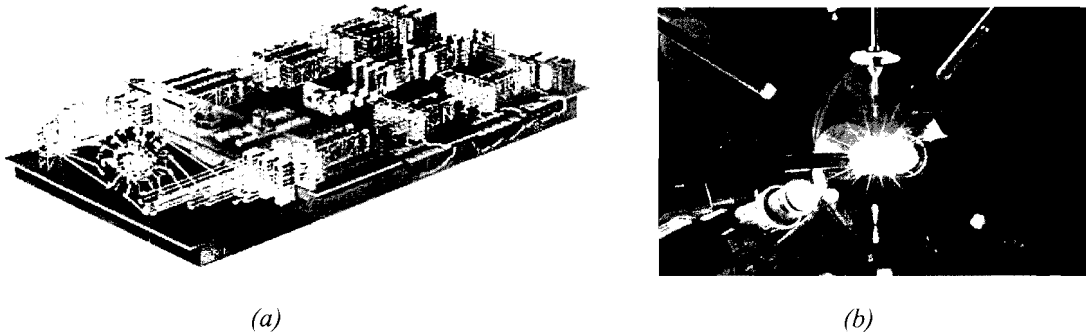


Figure 1: (a) 3-D Schematic view of the OMEGA system at LLE; (b) Illustration of the target system

1.3 The Fusion Reaction

Fusion is the joining together of small, light nuclei to form a larger, more massive nucleus. Since the incredibly powerful nuclear force is involved (as opposed to the electromagnetic force involved in chemical reactions) huge amounts of energy are released.

The final products in a fusion reaction weigh 0.7% less than the initial ingredients, thus 0.7% mc^2 is converted into energy: *One gram of fuel yields 175,000 kW-hours of energy* [3].

Fusion is the source of energy that powers the stars. In the center of a star, temperatures are so high and densities are so great that hydrogen atoms fuse together and release energy. Technologies such as laser-driven inertial confinement fusion attempt to recreate and harness the same reaction on earth. The technology would provide a clean, virtually limitless source of energy [4]. The fuel for fusion is provided by two isotopes of hydrogen: deuterium and tritium. Deuterium is widely available from seawater and is easily extracted. Tritium, on the other hand, is radioactive, with a half-life of 12.3 years; therefore tritium does not last long enough to be acquired in significant amounts naturally. Tritium is produced from lithium using the reaction:



The lithium absorbs the neutron and generates a tritium while releasing a bit more energy in the process. The D-T fusion reaction (see Fig. 2) is given as

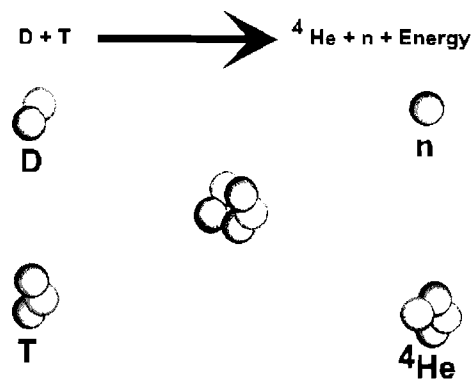
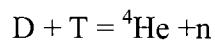


Figure 2: Illustration of the D-T fusion reaction.

The goal of fusion is to ignite the fuel so that atoms keep combining, releasing large amounts of energy -- many times more energy than the laser or source expended to start the reaction. A combination of high temperatures and densities is required to force positively charged nuclei together, but the resulting high pressure will tend to blow fusion plasma (hot ionized gas) apart. There are three ways of confinement – gravitational (occurring at astronomical scales); magnetic (employing very high magnetic fields) and inertial (using fuel inertia). The last is known as Inertial Confinement Fusion (ICF).

1.4 Inertial Confinement Fusion (ICF)

In the ICF method, a spherical capsule filled with fuel (deuterium and tritium) is bombarded with energy, compressing and heating a small region in the center of the fuel to allow the electrostatic repulsion of the nuclei to be overcome. The fusion reactions from this central “hot spot” deposit enough energy in the rest of the fuel that fusion occurs there too—this process is referred to as *ignition*. During the very short period of ignition (a fraction of a nanosecond) the fuel is pushed inward, so its own inertia acts to impede its disassembly; hence the term *inertial confinement fusion* [5,6].

To reach sufficient density to approach ignition conditions with reasonable laser power requires cryogenic targets with uniform fuel layer thickness and density, and a smooth inner surface finish. The major challenge for ICF target designers is to ignite a small mass of fusion fuel with a minimal amount of energy from a laser or accelerator, while maximizing the target gain--the ratio of driver energy input to fusion energy output.

It is critical that the target’s mount be of a material of low atomic mass – so that the implosion is minimally affected. Not only should the mount be able to support the target, but

also it should be able to absorb target vibrations. The elastic properties of spider silk are advantageous for supporting the ICF target.

1.5 Spider Silk

Silk is generally regarded as the proteinaceous filament secreted from glands present in some, but not all, invertebrates of the genera Arthropoda [7-9]. Silk production is a characteristic of all spiders and is also known among various mites, mantids, moths and beetles. Of all the silks investigated thus far, it appears that silk from the orb-weaving spiders possesses some of the most exceptional mechanical properties. The fibres of spider dragline silk possess a high tensile strength that is comparable to Kevlar and a high elasticity comparable to rubber.

The structure of spider silk can be pictured as a composite consisting of an amorphous low molecular weight matrix filled with nano-crystalline particles [10-11]. The mechanical properties of spider silk are determined by the genetic regulation of fibroin proteins and chemical and physical processing during spinning. Spider silk is completely biodegradable.

1.6 Application of Spider Silk in Inertial Confinement Fusion (ICF)

The mounting of a laser fusion target for ICF requires material of low atomic number to prevent X-ray emission that results from high-Z materials. In addition to a low mass, the material must possess favorable mechanical properties at cryogenic temperatures. The elastic properties of spider silk are highly suitable as the target mount. Silk mounts remain flexible and return to rest in a fraction of a second after a sharp impulse [12].

Targets at LLE are suspended by four strands of spider silk. Spider silk is an extremely strong and relatively flexible material by weight-basis. Its properties are similar to those of

Kevlar and steel – with a fiber diameter of $\sim 1.7\mu\text{m}$. Figure 3 shows a photograph of four spider silk strands holding a target.

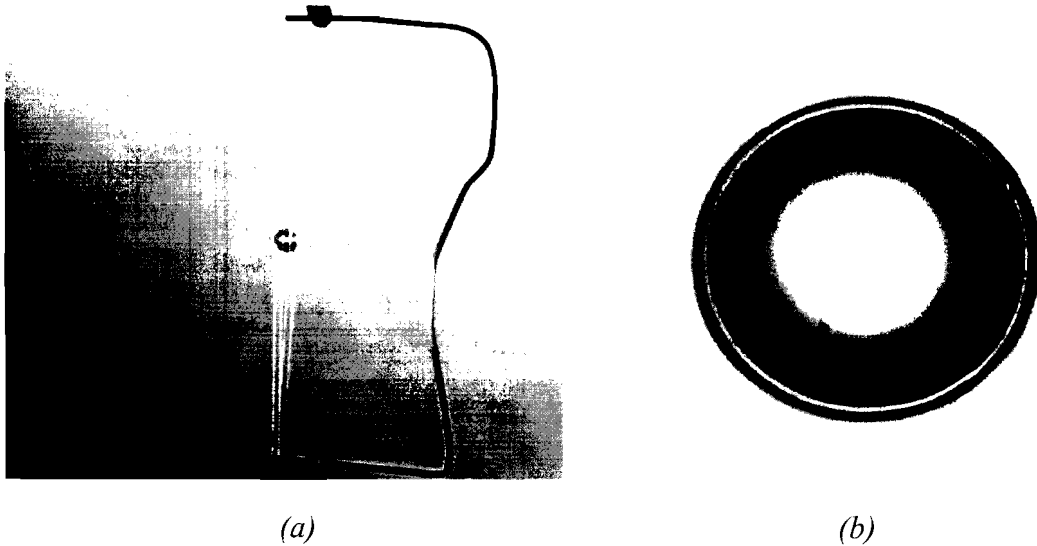


Figure 3: (a) Actual mount of 1mm diameter ICF target using four spider silk strands; (b) A D2 – gas filled target at cryogenic temperature ($\sim 18\text{K}$)

1.7 Mechanical Properties

This section provides a brief description of various important mechanical properties of materials discussed in this study [13].

Stress

The engineering stress on a material is defined as the **force per unit area** as the material is stretched (Figure 4). The cross-sectional area will change if the material deforms as it is stretched, so the area used in the calculation is the original undeformed cross-sectional area A_0 .

$$\sigma = \frac{\text{Force}}{A_0} \quad (1-1)$$

The units of stress are the same as those of pressure. The standard international unit for stress (pressure) is N/m^2 and is known as Pascal, (Pa). In the polymer literature, stress often is expressed in terms of psi (pounds per square inch). (1 MPa = 145 psi)

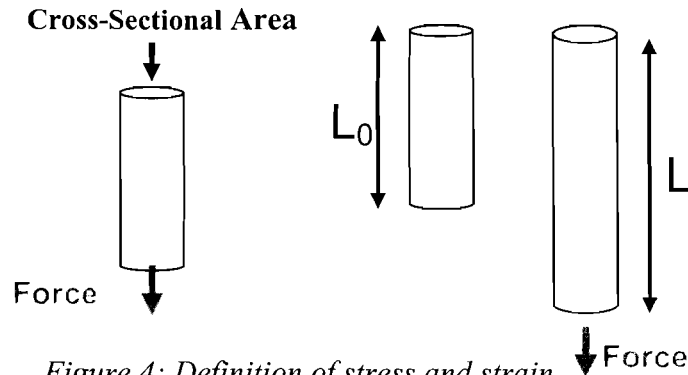


Figure 4: Definition of stress and strain

Strain

The strain is a measure of the change in length of the sample. The strain commonly is expressed as fractional change in length, $\Delta L/L_0$. Strain is a unitless number that characterizes the ductility of a material.

$$\varepsilon = \frac{L - L_0}{L_0} = \frac{\Delta L}{L_0} \quad (1-2)$$

Stress-Strain Curves

A tensile **stress-strain curve** is a plot of stress on the y-axis vs. strain on the x-axis. In the plot shown in Figure 5, strain is expressed as elongation. Stress-strain curves are measured with an instrument designed for tensile testing. It can be observed that as the strain (length) of the material increases, a larger amount of stress (force) is required. As the elongation is increased, the sample eventually breaks.

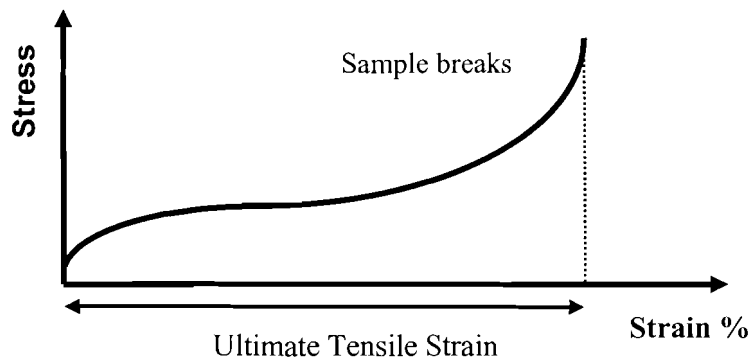


Figure 5: A typical stress-strain characteristics of a material. The area under the curve is the toughness and the strain at the break point is defined as the ultimate tensile strain (UTS)

Young's Modulus

The amount of force (F) applied is proportional to the amount of displacement (x) on an object, as defined in Hooke's law (with k being the spring constant).

$$F = - kx \quad (1-3)$$

Young's modulus (E) is derived from Hooke's Law, and is defined as the ratio of stress to strain in this linear region. It also is called the modulus of elasticity or the tensile modulus. Should a sample be loaded and unloaded in this region, it will return to its original length and cross sectional area.

$$E = \frac{\sigma}{\epsilon} \quad (1-4)$$

Stress-strain curves often are not straight-line plots, indicating that the modulus is changing with the amount of strain. In this case the initial slope usually is used as the modulus, as is illustrated in Figure 6. Rigid materials, such as metals, have a high Young's modulus. In general, fibers have high Young's modulus values, elastomers have low values, and plastics lie somewhere in between, as seen in Table I. The point at which the slope

deviates from linearity is known as the yield point [9]. At this point, the material is strained beyond its elastic region and will not return to its original state if unloaded.

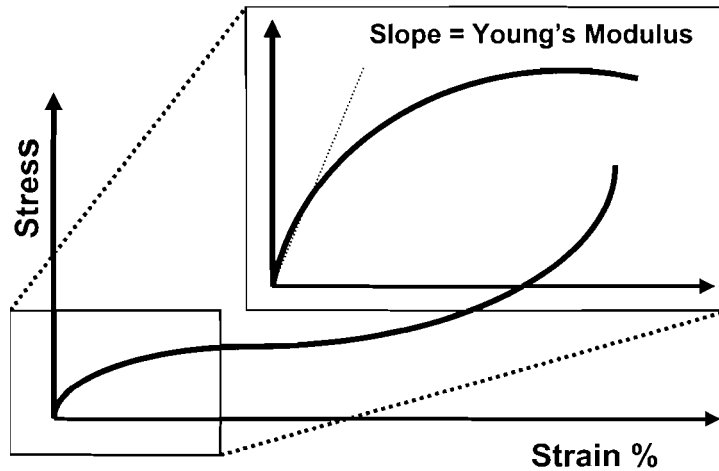


Figure 6: Young's modulus is the slope of a stress-strain curve in the linear regime

Tensile Strength

The tensile strength is the stress needed to break a sample. It is expressed in Pascals or psi (pounds per square inch). The tensile strength is an important property for materials that are going to be stretched. For instance, fibers must have strong tensile strength [9]. The maximum load defines the ultimate tensile strength (UTS) as

$$\sigma_{UTS} = \frac{P_{MAX}}{A_0} \quad (1 - 5)$$

where P_{MAX} is the maximum load and A_0 is the original cross-sectional area.

Energy to Break: Toughness

The energy it takes to rupture a sample is defined as the amount of energy required to break the sample per unit mass. It is given by the area under the load-displacement curve.

1.8 Mechanical Properties of Spider Silk

Table I lists important mechanical properties of spider silk in comparison to some other known materials [7]. Spider silk's mechanical properties are largely dependent on a high degree of molecular orientation, which has previously been demonstrated in both the crystalline and the amorphous domains of dragline silk. A spider's internal liquid crystalline spinning induces the high orientation of protein molecules [16-17].

Table I: Mechanical properties of spider silk in comparison to other materials [Ref 7]			
Material	Young's Modulus (GPa)	Tensile Strength (GPa)	Energy to Break (J/Kg)
Spider Silk	2.2*	1.2*	1×10^5
KEVLAR	100	4.0	3×10^4
Cellulose Fibers	30.0	0.8	9×10^3
High Tensile steel	200	3.0	1×10^3
Bone	20.0	0.2	3×10^3

* Values obtained in Bonino thesis [9]

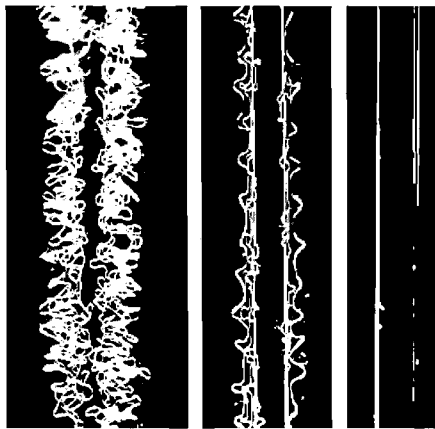


Figure 7: Spider silk shown as normal size, stretched 5 times and 20 times its original length [Reprinted from Ref. 18].

On a micro level, as the silk is loaded, the protein chains move along each other and become stretched out due to the load's force and the silk's elasticity (as depicted in Figure 7). This is the extraordinary property that makes silk very interesting scientifically.

II. OBJECTIVE

Measurement of Young's Modulus and Tensile Strength of spider silk was carried out at room temperature and at 100C, by Bonino [9]. The objective of the present study was to make these measurements at cryogenic temperatures. For this purpose, a high-precision thermal mechanical analyzer (TMA) needed to be set up and calibrated for measurements at room temperature and at 158K. Though the actual target temperature is held at nearly 20K, it was appropriate to test the physical properties at 158K based on the fact that physical properties do not change appreciably below the glass transition temperature, which is ~193K, for spider silk [19]. These quantitative results will assist the Lab in ICF modeling and further investigation.

III. EXPERIMENTAL

3.1 Silk sample

For the study presented here, a common brown spider, *Statoda Triangulosa* (Walckenaer) was chosen to produce silk. [9]. Its dragline silk was used for the experiments. Draglines are used to connect the spider to the web, as safety lines in case a spider should fall, and as the non-sticky spokes of the web. Dragline silk is the strongest kind of silk because it must support the weight of the spider. Silk samples were tested within two to eight days after being harvested. The diameter of the silk strand was determined using a LEO scanning electron microscope.

3.2 Sample Mounting

The spider silk was harvested in a class-500 cleanroom where the spiders were kept. To obtain the silk, the spider was dropped so it would generate its dragline fiber. A nonagon shaped spool with UV glue on each prong collected the strand – yielding nine separate

sections. Under a stereo microscope (50x) the silk was carefully glued to the TMA's upper chuck. A silicon carbide fiber with a diameter of 70 μm was glued onto the opposite end of the silk sample. Using the calibrated divisions of the microscope lens, the length of the sample was measured (between the glue points). Subsequently the sample was cut from the spool and the chuck was reattached to the TMA. The SiC fiber, which served as a plumb bob, was then glued to the bottom chuck (allowing for slack in-between), as shown in Figure 8(a). For tests at cryogenic temperatures, the TMA chamber was filled with liquid nitrogen vapor. Before cooling, the sample was purged with inert helium gas to prevent condensation. Tests were started once the system reached an equilibrium temperature.

3.3 Sample Testing

The PerkinElmer TMA utilized in this study is equipped with PYRIS™ software that runs the TMA and allows data capture and analysis. Figure 8 (b) shows a photograph of the test system and Figure 8 (c) is a close-up photograph showing the sample chamber. A uniaxial force pulled on the sample at the rate of 0.1mN/minute. As the force was applied, the system measured the displacement relative to the grip's initial position. To determine when the sample begins loading, the point where the slope abruptly changes is designated as the load point. Eventually a sharp increase in slope arises (the slope becomes nonexistent), which indicates that the silk has ruptured.

The stress-strain values were calculated using displacement and force values from the load point onward. The coordinates (force, displacement) at which the sample loaded were taken as the zero force and zero displacement. Strain was calculated and recorded. Ultimate tensile stress values were determined using the diameter obtained from the SEM micrographs.

Important mechanical properties have been extracted using the American Society for Testing and Materials (ASTM) standards. The ASTM standard D3822 defines the yield strength and yield strain at a point from where the initial slope of the stress-strain characteristics begins to deviate from linearity.

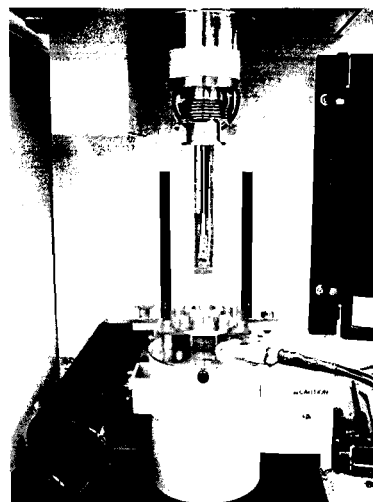
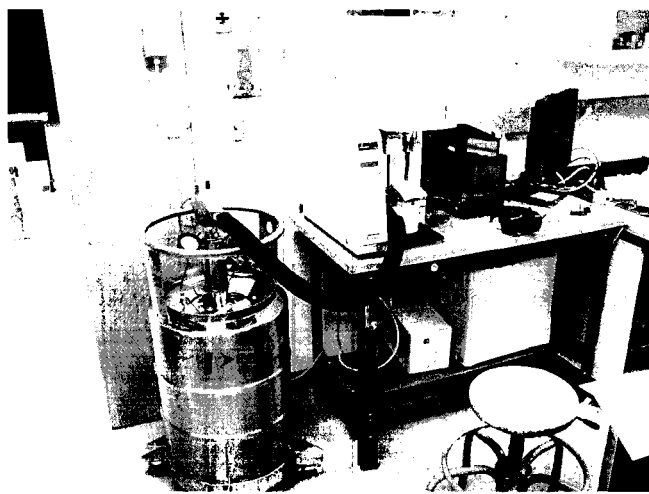
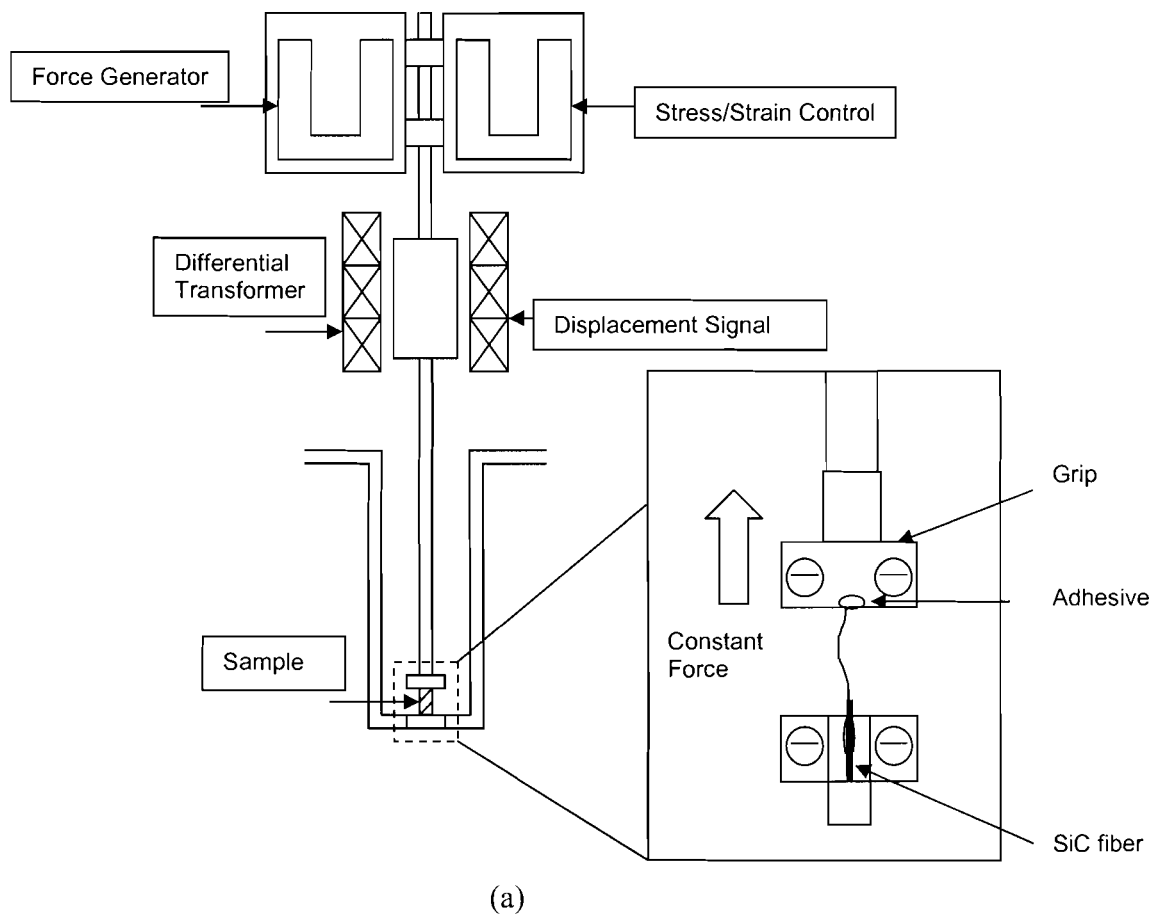


Figure 8: (a) Schematic of the thermal mechanical analyzer system; (b) and (c) actual photographs of the system showing liquid nitrogen cryostat and sample chamber.

IV. RESULTS AND DISCUSSION

4.1 Silk Diameter

Figure 9 shows an SEM micrograph of a typical silk strand tested in this study. Surprisingly, each batch of silk from the tested spider was actually a dual-stranded fiber. The average combined diameter of the five batches of silk was $1.84 \mu\text{m}$.

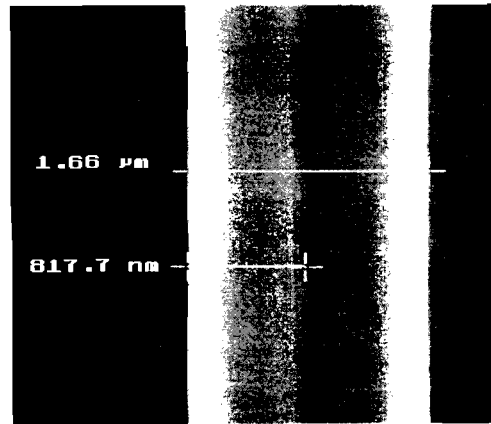


Figure 9: SEM micrograph of a typical silk strand tested in this study.

4.2 Stress-Strain Characteristics

Figure 10 shows a typical comparison between the force-strain values at different temperatures (room temperature and cryogenic).

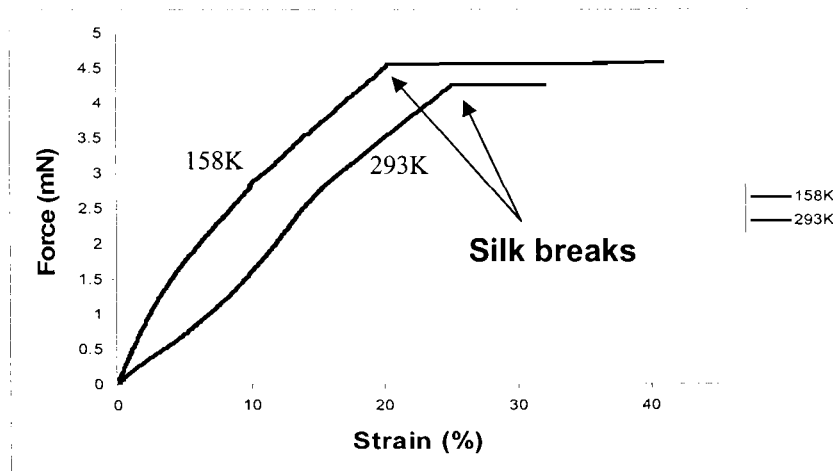


Figure 10: Force-strain characteristics of spider silk at 298K and 158K.

These values were determined from nine room temperature tests and nine cryogenic tests. The modulus values were extracted from such graphs for each run, by carefully measuring and calculating each initial slope. Figure 11 shows the statistical distribution of the modulus values.

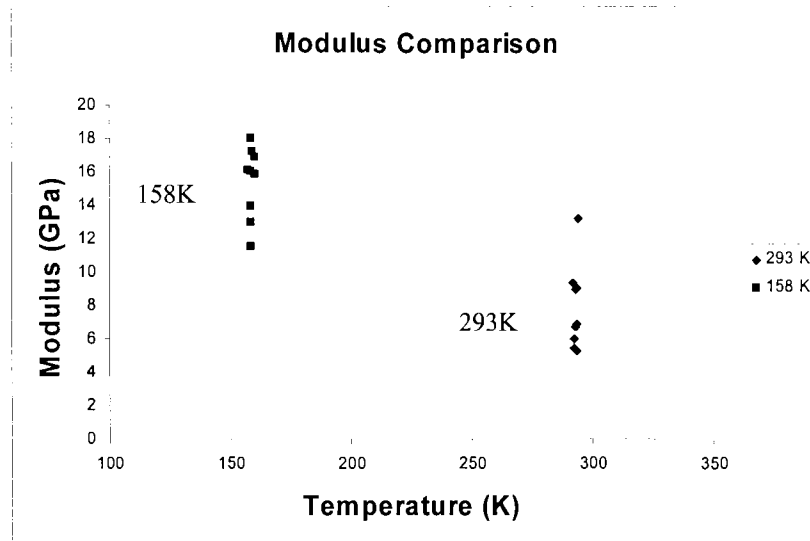


Figure 11: Modulus values obtained for different sample runs

Table II shows the final values for Young's modulus, ultimate tensile strength, and ultimate strain. It can be observed that the average UTS and ultimate strain were minimally affected, whereas the average modulus increased by a factor of two.

Table II. Measured Mechanical Properties		
Temperature	293K	158K
Average Modulus	7.9 GPa \pm 1.9 GPa	15 GPa \pm 1.6 GPa
UTS	1.7 GPa \pm 0.40 GPa	2.1 GPa \pm 0.01 GPa
Ultimate Strain	27 % \pm 8.00%	23% \pm 1.9%

V. CONCLUSIONS

The objectives of this experiment were met successfully. The goal of setting up and using the TMA was accomplished. Silk properties calculated at room temperature were in agreement with previous experiments. The effect of cryogenic temperatures was noted, producing little change in ultimate stress and ultimate strain, while doubling the stiffness of the silk (modulus). This change may be attributed to the composite structure of the silk. The crystalline components of the material may have become stiffer at lower temperatures due to a decrease in lattice energy. On the other hand, the change in the amorphous phase is minimal. In addition, the study reflects the resilience of spider silk over a wide range of temperature, which can be extended to various other applications of biomaterials. This data supports the continued use of spider silk as the premier mount for targets for ICF at LLE.

ACKNOWLEDGEMENS

The author would like to acknowledge Mr. Mark Bonino and Dr. David Harding of LLE for their guidance, advice, and mentoring. Special appreciation is due to Mr. Brian McIntyre of the UR Institute of Optics for SEM analysis. The author wishes to thank the entire LLE Microfabrication staff for their help and support. Lastly, the author is extremely thankful to Dr. Stephen Craxton for organizing the LLE High School Research Program.

REFERENCES

- [1] <http://www.lle.rochester.edu/>.
- [2] http://www.lle.rochester.edu/02_visitors/02_aboutomega.html.
- [3] F. Peterson, Department of Nuclear Engineering, University of California, Berkeley and the UCB Thermal Hydraulics Research Group, 1998;
http://www.nuc.berkeley.edu/thyd/icf/DT_fusion.html.
- [4] J.G. Delene, "Updated Comparison of Economics of Fusion Reactors," *Fusion Technology*, Vol. 19, pp. 807 (1991).
- [5] W.J. Hogan, Editor, *Energy from Inertial Fusion*, International Atomic Energy Agency, Vienna, Austria (1995) (457 pages).
- [6] John Lindl, *Physics of Plasmas*, **2**, 3933, (1995).
- [7] J. M. Gosline, M.E. DeMont and M.W. Denny, "*The Structure and Properties of Spider Silk*", *Endeavour*, New Series, Vol. 10, No.1, (1986).
- [8] F. Vollrath, "Spider Webs and Silks", *Scientific American*. March 1992, pp. 70-76.
- [9] M. Bonino, "*Material Properties of Spider Silk*", M.S. Thesis, University of Rochester, Rochester NY, 2003.
- [10] E. Oroudjev et al., "Segmented nanofibres of spider dragline silk: atomic force microscopy and single-molecule force spectroscopy", *PNAS Early Edition*, www.pnas.org/cgi/doi/10.1073/pnas.082526499.
- [11] <http://www.zoology.ubc.ca/labs/biomaterials/ab-paul.html>.
- [12] B.A. Brinker et al., "Inertial Fusion Target Mounting Methods: New Fabrication Procedures Reduce the Mounting Support Perturbation", *J. Vacuum Science and Technology*, A 1(2), April-June (1983), pp. 941-944.
- [13] <http://faculty.uscs.edu/llever/Polymer%20Resources/Mechanical.htm>; National Science Foundation's Division of Undergraduate Education through grants DUE #9950809 and DUE #9950.
- [14] Carraher, C. E., Jr *Polymer Chemistry: An Introduction*, 4th Ed., Marcel Dekker, NY: 1996. p. 120.
- [15] "Mechanical Properties of Polymers", : <http://www.psrc.edu/macrog//mech.htm> [2000, May 21].
- [16] F. Vollrath, Strength and structure of spider's silks, *Review in Molecular Biotechnology*. 2000, Vol. 74, 67-83.

[17] R. F. Foelix, Spider web, *Biology of spiders*. New York: Oxford University Press: Georg Thieme Verlag, 1996.

[18] E. Kullmann, H. Stern, Leben am seidenen Faden, Die rätselvolle welt der spinnen, 1975, Verlagsgruppe Bertelsmann Verlag, Munchen, Germany, ISBN 90 222 0239 9.

[19] Cunniff PM, Fossey SA, Auerbach MA, Song JW, Kaplan DL, Adams WW, Eby RK, Mahoney D, Vezie DL. *Polym Adv Technol* 1994;5:401.